# Pathway of Proton Uptake in the Bacteriorhodopsin Photocycle†

László Zimányi,‡,§ Yi Cao,‡ Richard Needleman,∥ Michael Ottolenghi,⊥ and Janos K. Lanyi*,‡

*Department of Physiology and Biophysics, University of California, Irvine, California 92717, Department of Biochemistry, Wayne State University School of Medicine, Detroit, Michigan 48201, and Department of Physical Chemistry, The Hebrew University of Jerusalem, Jerusalem 91904, Israel*

*Received March 29, 1993*

ABSTRACT: The time courses of chromophore reactions and proton uptake in the second half of the photocycle of the proton pump bacteriorhodopsin (BR) were examined. At pH >8.5, the kinetics are simplified by the fact that only the M and N intermediates accumulate. The relaxation kinetics after perturbation of M with a second, blue flash confirm that M ↔ N equilibration is the only significant cause of the biphasic M decay. With this feature, the analysis of time-resolved difference spectra yields a scheme which contains two sequential N states connected by a nearly unidirectional reaction. The proton uptake from the bulk, as measured with the pH-indicator dye pyranine, occurs during the decay of the first N rather than the recovery of BR. The results thus suggest the model $M_2^{(-1)} \leftrightarrow N^{(-1)} + H^+$ (from the bulk) $\leftrightarrow N^{(0)} \rightarrow BR$, where the superscripts indicate the protonation state of the protein relative to BR. $M_2^{(-1)} \rightarrow N^{(-1)}$ is reprotonation of the Schiff base from D96, $N^{(-1)} + H^+$ (from the bulk) $\rightarrow N^{(0)}$ is uptake of proton from the cytoplasmic side, and $N^{(0)} \rightarrow BR$ represents 13-cis to all-trans reisomerization of the retinal and other relaxations which regenerate the initial state. R227, a residue near D96, affects the deprotonation of D96 more than the subsequent proton uptake. According to the changed $[M_2^{(-1)}]/[N^{(-1)}]$ equilibrium in the R227Q protein, interaction between R227 and D96 is responsible for about 1 pH unit of the decrease in the $pK_a$ of D96 during the reprotonation of the Schiff base. According to the pH dependencies of the rate constants in the $N^{(-1)} \leftrightarrow N^{(0)}$ equilibrium in wild-type and R227Q, interaction with R227 lowers the $pK_a$ for proton uptake from the bulk by 0.5 pH unit, to 11. We conclude from the proton uptake kinetics that at physiological pH free energy is converted to proton electrochemical potential in this pump not only as protons are released on the extracellular side [Zimányi, L., Váró. G., Chang, M., Ni, B., Needleman, R., & Lanyi, J. K. (1992) *Biochemistry 31*, 8535–8543] but also as protons are taken up on the cytoplasmic side.

The intraprotein proton-transfer events in the photocycle of the light-driven proton pump bacteriorhodopsin consist of the protonation of residue D85 on the extracellular side by the retinal Schiff base and the subsequent reprotonation of the Schiff base by residue D96 on the cytoplasmic side [reviewed recently in Mathies et al. (1991), Rothschild (1992), Lanyi (1992), and Oesterhelt et al. (1992)]. The former is coupled to proton release at the extracellular surface from what appears to be a hydrogen-bonded complex which includes R82, Y57, and probably bound water (Braiman et al., 1988; Váró et al., 1992; Brown et al., 1993a),[1] while the latter is coupled to proton uptake at the cytoplasmic surface which reprotonates D96. These four events complete the circuit of the proton across the protein. The photocycle contains spectroscopically distinct intermediates designated as J, K, L, M, N, and O,[2] and several of their substates, arising and decaying in sequence. The chromophore reactions associated with proton release in the first half of the photocycle are described by Zimányi et al. (1992) as $M_1^{(0)} \rightarrow M_1^{(-1)} + H^+$ (to the bulk) $\rightarrow M_2^{(-1)}$. Thus, the transported proton is released on the extracellular side after proton transfer from the Schiff base to D85. Since the $pK_a$ of the release complex is lowered to about 6 at this time in the cycle, at physiological pH (between 7 and 8) free energy will be dissipated upon dissociation of the proton. It is this free energy which is conserved as the increased chemical and electrical potential for protons in the extracellular bulk phase in illuminated intact cells or envelope vesicles.

The events in the second half of the photocycle are less clear. Neither the absorption spectra of N and O nor their kinetics have been firmly established from time-resolved absorption measurements. One of the reports (Váró & Lanyi, 1991a) calculated a spectrum for N which resembled earlier estimates (Kouyama et al., 1988; Dancsházy et al., 1988), but since the O state did not accumulate in large amounts, its calculated spectrum was of necessity an approximation only. The kinetics from the time-resolved spectra in the visible (Váró & Lanyi, 1991a,b), as well as from FTIR (Gerwert et al., 1990; Souvignier & Gerwert, 1992) and resonance Raman (Ames & Mathies, 1990), were consistent with the scheme M ↔ N ↔ O → BR. An important feature of this kind of model is the M ↔ N equilibration, introduced originally to explain the biphasic M decay (Otto et al., 1989). Both M ↔ N and N ↔ O equilibration reactions are supported by the pH (Otto et al., 1989; Váró & Lanyi, 1990b; Ames & Mathies,

† This work was supported by grants to J.K. L. from the National Institutes of Health (GM 29498), to R.N. from the National Science Foundation (MCB-9202209), the U.S. Army (DAAL03-92-G-0406), and the U.S. Department of Energy (DEFG02-92ER20089), and to L.Z. from the National Scientific Research Fund of Hungary (OTKA T5073).

* To whom correspondence should be addressed.

‡ University of California.

§ Permanent address: Biological Research Center of the Hungarian Academy of Sciences, Szeged, Hungary.

∥ Wayne State University School of Medicine.

⊥ The Hebrew University of Jerusalem.

[1] Brown, Cao, Needleman, and Lanyi, unpublished results.

[2] Abbreviations: J, K, L, M, N, and O are the photointermediates of the bacteriorhodopsin photocycle; BR is the initial state. Superscripts, where given, refer to the net protonation of the protein relative to the initial state. Subscripts for M substates refer to pre- and postswitch states [$M_1$ and $M_2$, cf. Váró and Lanyi (1991a,b)]. CAPS is 3-(cyclohexylamino)-1-propanesulfonic acid; Bis-Tris-propane is 1,3-bis[tris(hydroxymethyl)methylamino]propane.

0006-2960/93/0432-7669$04.00/0 

1990) and temperature (Chernavskii et al., 1989; Váró & Lanyi, 1991b; Chizhov et al., 1992) dependencies of the rate constants. This single-cycle scheme is disputed in some recent reports, however. The alternative models proposed are fundamentally different since they contain, as suggested earlier (Hanamoto et al., 1984; Diller & Stockburger, 1988; Dancsházy et al., 1988; Bitting et al., 1990), two independent M to BR pathways. They place the beginning of the recovery of bacteriorhodopsin either before the decay of N, requiring a separate direct M → BR pathway (Tokaji & Dancsházy, 1992b), or well after the decay of M states (Fukuda & Kouyama, 1992a,b). In the latter version of this model, the slower decay component of M arises from photoreaction of the N intermediate (Kouyama et al., 1988; Fukuda & Kouyama, 1992b). What these models have in common is that M decays by unidirectional reactions. For this reason, the recent demonstration of significant thermal N to M back-reaction by two-flash experiments (Druckmann et al., 1993) argues strongly against them. Likewise, the two-photon model is contradicted by several reports in which the photoproduct of N is red-shifted rather than strongly blue-shifted as M would be (Váró & Lanyi, 1990b; Balashov et al., 1990; Tokaji, & Dancsházy, 1992b; Yamamoto et al., 1992). Although we find that M is produced in the photoreaction of N under some conditions, it is not produced under the conditions where the biphasic M decay is usually measured (Brown et al., 1993b).

The reactions which lead to the accumulation of the O state are even more problematical. When followed by resonance Raman (Ames & Mathies, 1990), the pH dependence of the amount of O was accounted for by a steep decline of the rate of the N → O reaction with increasing pH above 7, while the O → BR reaction was constant. This is as expected if in this pH range proton uptake by D96 began to limit the rate of N decay. However, when followed by absorption at 700 nm (Eisfeld & Stockburger, 1992), the rise of O was only slightly pH dependent, and it was its decay instead which was greatly slowed with increasing pH. This is in conflict not only with the other report but also with the decreased accumulation of O at increasing pH. Further, measuring these rates with the fluorescence of O (Ohtani et al., 1992) revealed no strong pH dependency in either the rise or the decay of O, up to pH 9.3. As for the proton uptake on the cytoplasmic side which completes the transport cycle, it appears to lag sufficiently behind the decay of M to associate it with the decay of N (Skulachev et al., 1988; Váró & Lanyi, 1990a), but the uncertainties of the kinetics of N and O make this a somewhat tentative assignment. The validity of the $N^{(-1)} + H^+$ (from the bulk) ↔ $O^{(0)}$ → BR scheme depends, in fact, mostly on FTIR spectra which show that the 1742-$cm^{-1}$ negative band due to the deprotonated D96 decays together with other bands characteristic of N (Braiman et al., 1991; Gerwert et al., 1990; Souvignier & Gerwert, 1992).

In this report, we attempt to describe the kinetics of the M to BR chromophore reaction pathway and identify the step in which proton is taken up from the bulk. To circumvent the problems with the O intermediate, we examine the simpler case where O does not accumulate, i.e., pH >8.5. The results confirm that there is equilibration between M and N (Druckmann et al., 1993), and rule out multiplicity of M to BR pathways as the cause of the observed biphasic M decay. The chromophore kinetics and the proton uptake kinetics both indicate that there are two sequential N substates. The events in the second half of the cycle at pH >8.5 are described by the scheme: $M_2^{(-1)} \leftrightarrow N^{(-1)} + H^+$ (from the bulk) ↔ $N^{(0)}$ → BR. The uptake of the proton is at a sufficiently high $pK_a$ (about 11) to make the $N^{(-1)} \rightarrow N^{(0)}$ reaction much faster than its back-reaction at any physiological pH. The rate constants for the R227Q protein indicate that interaction between D96 and R227 affects the internal proton transfer in the $M_2^{(-1)} \leftrightarrow N^{(-1)}$ reaction more than the proton uptake from the bulk in the $N^{(-1)} + H^+ \leftrightarrow N^{(0)}$ reaction which follows.

## MATERIALS AND METHODS

The *Halobacterium halobium* strain which produces recombinant R227Q bacteriorhodopsin was constructed as described before (Ni et al., 1990; Needleman et al., 1991). This mutant and the wild-type bacteriorhodopsin were isolated from *H. halobium* as purple membranes by a standard method (Oesterhelt & Stoeckenius, 1974). All spectroscopy was with purple membranes encased in polyacrylamide gels and equilibrated with the desired buffer or salt solutions as described before (Needleman et al., 1991).

The two-flash experiments were with right-angle geometry, where the first flash was from a frequency-doubled Ne-Yag laser (532 nm, 7-ns duration) at 90° from the measuring beam, while the second flash was from a nitrogen-pumped dye laser (406 nm, 0.5-ns duration) at 270°. The same arrangement but with the Ne-Yag laser only was used also for measuring absorption changes at single wavelengths, and for measuring proton release and uptake with the pH-indicator dye pyranine (Cao et al., 1993). The instrument in these experiments was the one described before (Váró & Lanyi, 1990a) except that the measuring light passed through an additional monochromator between the sample and the detector, and signal-averaging was with a Thurlby Digital Storage Adaptor Model 524. The time scale was linear, and included 1024 points in each of several overlapping time segments. In some cases, the data were converted to logarithmic time scale with a program written by G. Váró (Biological Research Center of the Hungarian Academy of Sciences, Szeged, Hungary) which also reductively averaged the points.

For the time-resolved spectral measurements, the nitrogen-pumped dye laser was used, but tuned to 580 nm. The rest of the instrumentation and the data analysis for the optical multichannel spectroscopy is described elsewhere (Zimányi et al., 1989; Zimányi & Lanyi, 1993). Noise was removed from the spectra by reconstructing the data from its significant SVD components.

Models were fitted to the data with either discrete rate constants as before (Váró & Lanyi, 1991a; Zimányi & Lanyi, 1993) or distributed rate constants, with a program for Runge–Kutta numerical integration, SIMULATE, written by one of us (L.Z.). For distributed kinetics, a range of values was calculated for each rate constant around a suitable mean by multiplying with $e^x$, where $x$ assumed 11 equidistant values between $-\Delta$ and $+\Delta$. Values of $\Delta$ from 0.5 to 1 were found to produce improved fits over discrete kinetics. Each of the rate constants in this range was then assigned, randomly, to 28 subpopulations of bacteriorhodopsin, with frequencies around the mean according to a Gaussian. The fit of the model was the sum of the fits of the 28 subpopulations.

## RESULTS

*Kinetic Relationship of M to N.* The existence of an N to M back-reaction was recently demonstrated by perturbing the M kinetics with a second, near-UV flash (Druckmann et al., 1993). This method makes use of the fact that the chromophore in the M state can be reconverted to BR by blue light (Kalisky et al., 1978, 1981; Druckmann et al., 1992). Because the thermal steps in this reconversion are with

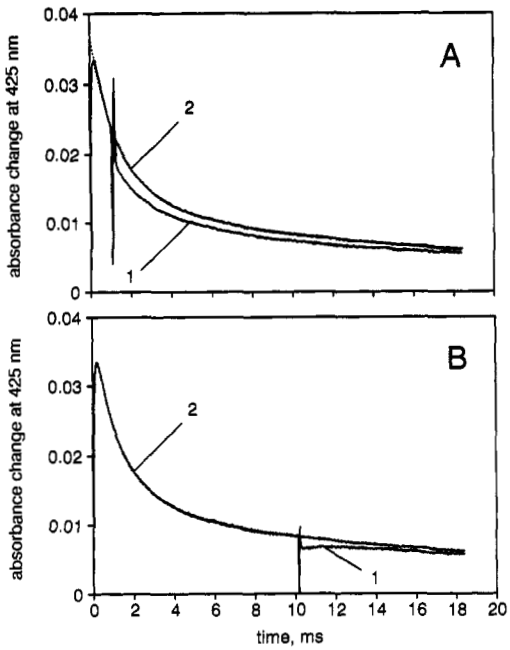


FIGURE 1: Transient absorption change at 425 nm, which detects the M intermediate, in two-flash experiments. At time = 0, the bacteriorhodopsin was photoexcited by a 532-nm flash, followed by partial depletion of the M photointermediate by a second, 406-nm flash at (*A*) 1 ms or (*B*) 10 ms (trace 1). These traces were obtained by subtracting controls with the second flash only (multiplied by 1 *minus* the photocycling fraction), as described in Druckmann et al. (1993). The validity of this subtraction was ascertained by varying the relative intensities of the first and second flashes (not shown). Superimposed on the first flash only control (trace 2) in (*A*) is the best fit of the model M ↔ N → BR (dashed line, $k_1$ = 550 $s^{-1}$, $k_{-1}$ = 132 $s^{-1}$, and $k_2$ = 82 $s^{-1}$). Conditions: 22 μM bacteriorhodopsin, 0.1 M NaCl, 50 mM Bis-Tris-propane, pH 9.5, 25 °C.

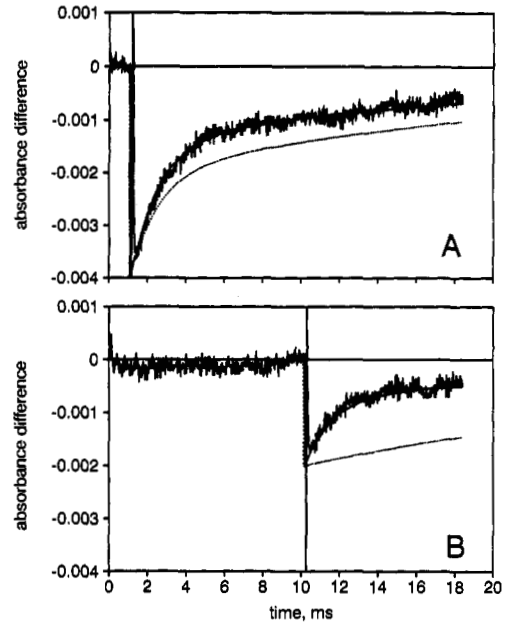


FIGURE 2: Effect of a second, 406-nm flash on the kinetics of the resumed M decay. The traces in (*A*) and (*B*) correspond to the 1- and 10-ms experiments in Figure 1, with the first flash only control trace subtracted from the two-flash traces. Solid lines: predictions of the M ↔ N model using the rate constants which give the fit to the control trace in Figure 1A. Dashed lines: predictions of the two independently decaying M states model using the rate constants and a ratio for the initial concentrations of the M states from a fit of similar quality to the control trace as the other model (not shown, $k_1$ = 670 $s^{-1}$, $k_2$ = 38 $s^{-1}$, amplitude ratio (0.66). For the calculations, see the Appendix.

submicrosecond kinetics, the depletion of M is essentially instantaneous on the millisecond time scale. The time course of the decay of the remaining M will thus provide information about the reactions involving M and N. Figure 1A,B shows kinetics for M produced by a 532-nm flash at zero time as measured at 425 nm. At 1 ms (A) and 10 ms (B) after this flash, a second, 406-nm flash depleted M by about 20%, and altered the further decay of M.

Figure 2A shows the difference between the 1-ms two-flash trace and the control trace with the first flash only; Figure 2B contains the same difference trace for the 10-ms experiment. First, the predictions of two simple kinetic schemes were compared with the data. Model A attributes the well-known and controversial biphasic M decay (e.g., Figure 1) to back-reaction from N with a significant rate, in the scheme M ↔ N → BR. Model B attributes the biphasic M decay to two M states, $M_{fast}$ and $M_{slow}$, which decay independently from one another and *via* unidirectional reactions. Either of these models fits the single-flash trace satisfactorily; the dotted line in Figure 1A is for model A. For model A, this fit defines three rate constants; for model B, two rate constants and the initial amounts of $M_{fast}$ and $M_{slow}$, $c^f$ and $c^s$. These parameters, *plus* an M depletion, $\Delta M$, of suitable magnitude, were used to generate curves (cf. Appendix) for comparison with the data in Figure 2. For evaluating the 1-ms experiment in terms of model B, the additional assumption was made that the quantum yields of the blue flash reconversion of the putative $M_{fast}$ and $M_{slow}$ are the same. The good proportionality between $\Delta M$ and the total concentration of M at the time of the second flash, in spite of the widely changing relative amplitudes of the fast and slow components, justifies this assumption. However, since by 10 ms $M_{fast}$ will have decayed virtually to zero, at 10 ms this becomes a moot point as the second flash can deplete $M_{slow}$ only. The predictions of model A agree remarkably well with the data from both 1- and 10-ms experiments (Figure 2). The predictions of model B disagree with both. The 10-ms experiment is particularly revealing. In model B, once $M_{fast}$ had decayed the resumed M kinetics can be only with the time constant of $M_{slow}$ (eq 5), but the measured data contain both fast and slow time constants (Figure 2B).

A combination of models A and B would have two independent M states, with either one or both in equilibrium with N. Closer examination of the data distinguishes between this mixed model and model A. In the analytical solution of model A (eq 2 and 3), the time courses of the difference traces (in Figure 2) are described by the decay of M without the second flash (in Figure 1) regardless of the delay between the two flashes. The only change with delay time is the amplitude of $\Delta M$. In contrast, in the mixed model where the ratio of $M_{fast}$ and $M_{slow}$, and therefore their contribution to M depletion, changes with time, the time course will be also dependent on the delay (eq 6). For this comparison, therefore, the data at 1 and 10 ms in Figure 2, as well as a third difference trace measured at 2 ms, were shifted to zero time and scaled to the initial amplitude of M accumulation. The single-flash M decay was inverted and superimposed (dashed lines) on these traces. Figure 3A shows very good agreement of the data with the initial M decay kinetics at each delay, i.e., with the prediction of model A. The existence of parallel M to BR pathways is thereby ruled out as a significant cause of the biphasic M decay kinetics under these conditions.

A third possible alternative, model C, would be the photoproduction of a slowly decaying M state from N. In this model, it is the measuring light which drives what we detect in Figures 2 and 3 as an N to M back-reaction. Although

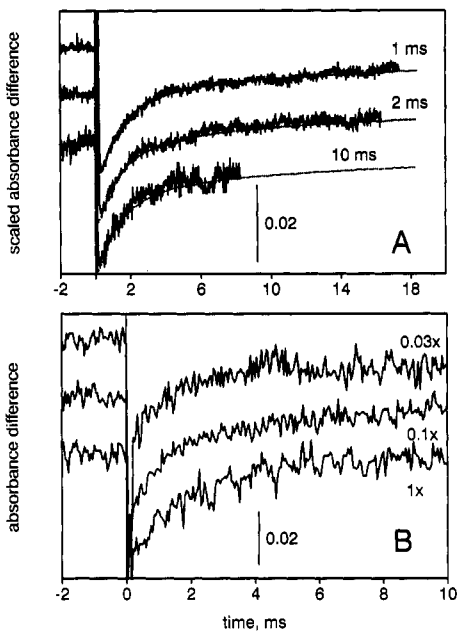


FIGURE 3: (*A*) Effect of the delay before the second flash on the time course of the resumed M decay. The 1- and 10-ms traces are from Figure 2, but scaled to the control (first flash only) M decay (lines 2 from Figure 1, multiplied by −1) and shifted to zero time. The trace labeled as 2 ms is from the same experiment but with 2-ms delay. Dashed lines: the control trace. (*B*) Effect of the intensity of measuring light on the resumed M kinetics. The three traces are equivalent to the 10-ms trace on Figure 2B, but the intensity of the measuring beam was attenuated to 10% and 3% of the normal value, as indicated. In both (*A*) and (*B*), zero time refers to the time of the second flash.

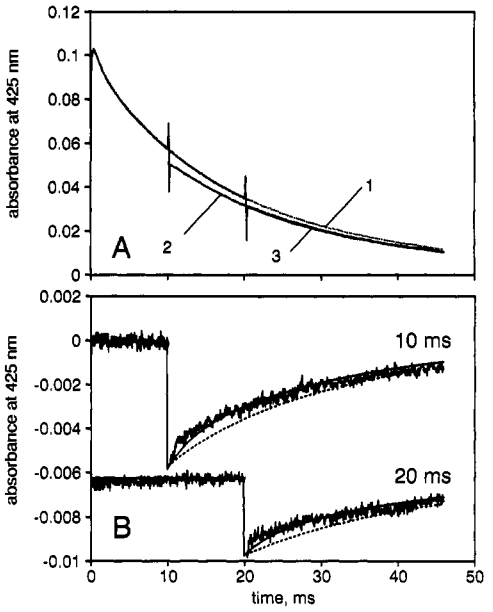


FIGURE 4: Effect of a second, 406-nm flash on the kinetics of the resumed M decay in R227Q bacteriorhodopsin. (*A*) Absorbance change at 425 nm with the first flash only (line 1, dashed), with the second flash at 10 ms (line 2) and 20 ms (line 3). The latter two were obtained by subtracting controls as in Figure 1A. (*B*) Two-flash *minus* first flash only traces for 10- and 20-ms delays. Solid lines: predictions of the M ↔ N → BR model using the rate constants which give the fit to the control trace in Figure 1A. Dashed lines: predictions of the two independently decaying M states model. Conditions: 22 μM R227Q bacteriorhodopsin, 0.1 M NaCl, 50 mM Bis-Tris-propane, pH 9.5, 25 °C.

the extinction of N is small at 425 nm (Dancsházy et al., 1988; Váró & Lanyi, 1991a; Fukuda & Kouyama, 1992b), where these measurements were made, this alternative was considered also. According to model C, the rate at which the original photoequilibrium between N and M is reestablished after the second flash should be linearly dependent on the intensity of the measuring light. Figure 3B shows difference traces between the data with the second flash at 10 ms and the single-flash control (as in Figure 1B but with the time of the second flash given as zero), at 100, 10, or 3% of the original measuring light intensity. Neither the double-flash M decay kinetics (Figure 3B) nor the single-flash kinetics (not shown) were influenced significantly by the measuring light within a 30-fold intensity range. Under the conditions of these experiments, therefore, the N to M reaction detected after the second flash is not a photoreaction driven by the measuring light. We present additional data in other reports (Druckmann et al., 1993; Brown et al., 1993b) which demonstrate that under these conditions blue light excitation of the N intermediate does not produce an M-like state.

Because the amount of BR photolyzed by the two flashes is greater than with the second flash alone, the M decay kinetics will have been altered somewhat by a cooperative effect (Tokaji & Dancsházy, 1992a). We have also observed such effects of flash intensity on M decay (not shown). For this reason, we performed subtractions, both as in Figure 1 and at a lower first flash intensity, also by using M decay traces extrapolated to the combined photocycling ratios in the double-flash experiments. Although this changed the net traces slightly, their overall features were not altered.

The structure predicts that R227, a residue near D96, is in the proton channel (Henderson et al., 1990). An effect of this arginine on proton transfer from D96 is suggested by the slowed decay of M in the R227Q protein (Stern & Khorana, 1989; Lin et al., 1991). Figure 4A (dashed line) shows the absorption change up to 50 ms at 425 nm in R227Q. When fitted with two exponentials, the relaxation time constant of the fast phase of M decay is slower than wild-type, while that of the slow phase is unchanged.[3] Depletion of M by a second, blue flash at 10 or 20 ms is followed by some recovery (Figure 4B) as in wild-type, but the difference between models A and B is small. The reason for this is that the calculated rate constants (cf. below) predict a much decreased amount of N in equilibrium with M, and consequently much less back-reaction.

*Photocycle Kinetics at pH 9.5.* We have recently developed a method for calculating the component spectra and the kinetics from a set of time-resolved difference spectra in the bacteriorhodopsin photocycle (Zimányi & Lanyi, 1993). This method takes advantage of the simplicity of the photocycle of the recombinant D96N protein, where the N and O intermediates do not accumulate and in a grid-search all potential solutions for the K ↔ L ↔ M sequence can be evaluated. We extend this method now for the wild-type photocycle at a high enough pH where the O state does not accumulate and thus only one additional intermediate, N, is present. Our strategy was to solve the first half of the cycle in the way it was done previously,

[3] The $\tau_1$ values for M decay in wild-type and R227Q are 1.5 and 6.3 ms, respectively, and the $\tau_2$ values are 26 and 24 ms (with amplitude ratios of 66:34 in wild-type and 22:78 in R227Q). This is the opposite of what was reported for the photocycle of the R227Q mutant when expressed in *Escherichia coli* (Lin et al., 1991). In that system, $\tau_1$ was unchanged from wild-type, but $\tau_2$ became 5 times slower. As for other differences between recombinant bacteriorhodopsins expressed in *H. halobium* and *E. coli* (Needleman et al., 1991; Váró et al., 1992), the causes of the discrepancy may be (a) that in the homologous expression system the protein is folded and assembled into the purple membrane lattice *in vivo*, while in the heterologous system it has to be refolded *in vitro* and a lattice probably does not form, and (b) that the surface potential of the detergent micelles usually used with the heterologously expressed protein is not as negative as in the purple membrane.

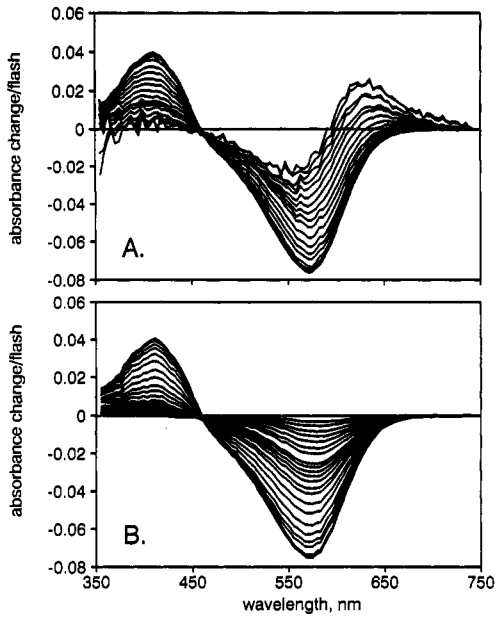


FIGURE 5: Time-resolved difference spectra after photoexcitation of bacteriorhodopsin at pH 9.5. (*A*) Rising phase; (*B*) falling phase of absorbance changes. Delay times in (*A*): 70 ns, 100 ns, 150 ns, 210 ns, 310 ns, 450 ns, 650 ns, 940 ns, 1.4 μs, 2 μs, 2.9 μs, 4.2 μs, 6 μs, 8.8 μs, 13 μs, 18 μs, 27 μs, and 39 μs. Delay times in (B): 56 μs, 81 μs, 120 μs, 170 μs, 250 μs, 360 μs, 520 μs, 760 μs, 1.1 ms, 1.6 ms, 2.3 ms, 3.3 ms, 4.9 ms, 7 ms, 10 ms, 15 ms, 21 ms, 45 ms, 65 ms, 94 ms, 140 ms, 200 ms, and 290 ms. Conditions: 21 μM bacteriorhodopsin, 100 mM NaCl, 50 mM CAPS, pH 9.5, 22 °C.

and use the derived spectrum of M and the amount of bacteriorhodopsin which photocycles in solving the second half.

Figure 5A,B shows the time-resolved difference spectra at pH 9.5. These spectra were fitted with spectra for K, L, and M calculated from a similar experiment but at pH 7 [as in Zimányi and Lanyi (1993)] and shown in Figure 6A. They are very similar to the earlier calculated spectra for the D96N protein (Zimányi & Lanyi, 1993). Figure 6B (points) shows the calculated transient concentrations fo K, L, and M.

Scaled amounts of the calculated difference spectrum for M were then subtracted from each of the measured spectra between 3.3 ms, by which time L will have decayed, and the end of the cycle. The criterion for the subtraction was that any absorption change in the 400-nm region, which is far removed from the absorption bands of species other than M, be eliminated. This assumes that in the 400-nm region the absorbance of states with a protonated Schiff base is not greatly different[4] from that of BR (Zimányi & Lanyi, 1993), as demonstrated indeed in several attempts to calculate difference spectra for N (Dancsházy et al., 1988; Fukuda & Kouyama, 1992b). Important for the further analysis, we find that the net difference spectra which remain after the subtraction (Figure 7) (a) are time-invariant between 3.3 and 10 ms and (b) decay to zero with a constant shape afterward. These features indicate that up to 10 ms no BR had recovered and that the net spectra include only BR and one other spectral entity. The latter conclusion was supported by the fact that the net spectra (Figure 7) were nearly identical in particular to scaled spectra at 140 ms and later, where the lack of an absorption increase near 400 nm had indicated the absence of M even before the subtraction. We conclude that the net

[4] The extinction of N near 400 nm is in fact somewhat lower than that of BR (Brown et al., 1993b), but this makes a negligible difference in these calculations.

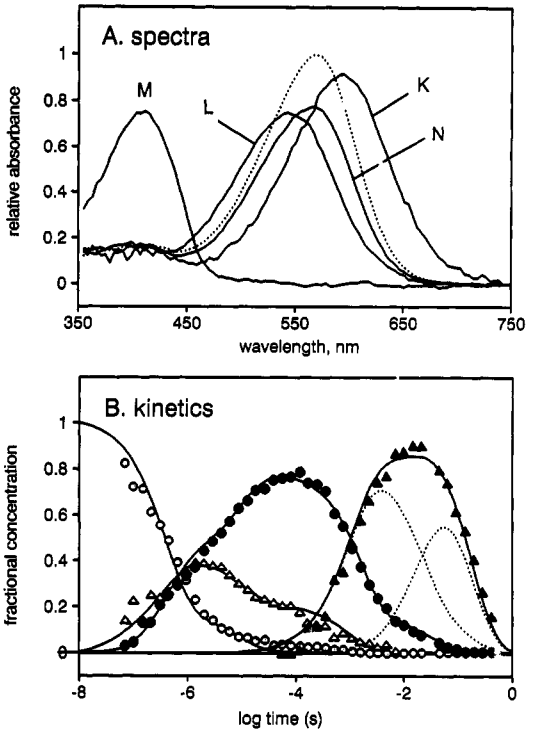


FIGURE 6: Derived spectra for the photocycle intermediates (*A*) and their kinetics (*B*). The data are from Figure 5. Details are given in the text. In (*A*), the dotted line is the spectrum of BR for comparison. In (*B*), the points are the calculated transient concentrations of the intermediates: (○) K; (△) L (total); (●) M (total); (▲) N (total). The solid lines are fits of the model, as explained in the text. The dotted lines indicate the predicted concentrations of the two N substates. The rate constants for the $M_2^{(-1)} \rightarrow N^{(-1)}$, $N^{(-1)} \rightarrow M_2^{(-1)}$, $N^{(-1)} \rightarrow N^{(0)}$, $N^{(0)} \rightarrow N^{(-1)}$, and $N^{(0)} \rightarrow$ BR reactions were 667, 111, 33, 5, and 6.7 $s^{-1}$, respectively.

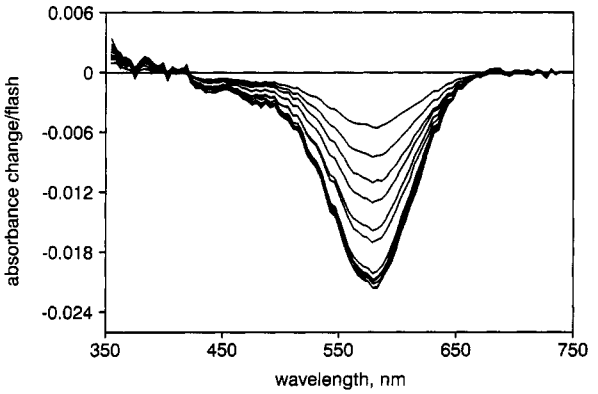


FIGURE 7: Time-resolved spectra for the second half of the photocycle, with the contribution of M removed. From spectra in Figure 4, scaled M *minus* BR spectra were subtracted so as to eliminate any absorption change near 400 nm. They are displayed as $(a - xb)/(1 - x)$ where $a$ is the measured spectrum, $x$ is the fractional concentration of M, and $b$ is the M *minus* BR difference spectrum. The spectra are for delay times 3.3, 4.9, 7, 10, 15, 21, 45, 65, 94, 140, and 200 ms.

spectra in Figure 7 are N *minus* BR spectra. The spectrum of N was calculated from the spectra between 3.3 and 10 ms in Figure 7 and the amount of photoexcited BR estimated from the first half of the cycle (8.9%). It is shown in Figure 6A. Its maximum is at 564 nm, which is a few nanometers to the red from those in earlier attempts to define N, and its amplitude relative to BR is 0.77, which is somewhat higher than in previous reports.

The transient concentrations in the second half of the cycle were then calculated (Figure 6B, points). Because the

extinction of N is high, the N *minus* BR difference spectrum has a small amplitude, and therefore the concentration of N is higher than suspected earlier. By 10 ms, N accumulates in amounts which exceed the maximum accumulation of M. As in other reports (Dancsházy et al., 1986; Tokaji & Dancsházy, 1992b; Fukuda & Kouyama, 1992a,b), we find that the decay of N is significantly delayed relative to the slower phase of the decay of M. After 140 ms, therefore, virtually the only photointermediate present is N. This would be consistent with a single M state and back-reaction from N if (a) there were two sequential N species with virtually the same spectra and (b) they were connected with a reaction strongly biased in the forward direction. For the first half of the cycle, up to $M_2^{(-1)}$, we used the scheme which fit the D96N protein, using two L states suggested (Zimányi & Lanyi, 1993) to account provisionally for the unusally delayed L decay in the wild-type sample. For the second half, we used the scheme $M_2^{(-1)} \leftrightarrow N^{(-1)} \leftrightarrow N^{(0)} \rightarrow BR$, where the rate of the $N^{(0)} \rightarrow N^{(-1)}$ back-reaction is small compared to the forward reaction. The fit to the points (not shown) was about as good as what we report elsewhere in such modeling (Váró & Lanyi, 1991a,b; Zimányi & Lanyi, 1993); i.e., small but persistent deviations occurred at times where the curvature of the concentrations was greatest.

Significantly improved fits were obtained when the rate constants were *distributed* rather than *discrete* values. The rationale for distributed kinetics is that the protein exists as an ensemble of subpopulations, each with a somewhat different conformation. Thus, the internal barriers, in this case to the photocycle reactions, are described by a probability distribution around a mean. For simplicity, one must assume that the parameters which determine this distribution are the same for all of the reactions. Nevertheless, distributed kinetics have been reported to give improved fits for a variety of kinetic data for bacteriorhodopsin (Váró & Keszthelyi, 1983; Groma & Dancsházy, 1986; Holz et al., 1988). The kinetics in Figure 6B were fitted therefore with a distribution of rate constants. For this calculation, the protein was divided into 28 subpopulations. The 11 particular values assumed by each of the rate constants in the model, with ranges determined by a maximal conformational free energy variation of $\pm\Delta kT$, with $\Delta = 0.7$, around a mean (cf. Materials and Methods), were randomly assigned to the 28 subpopulations according to a Gaussian distribution. The lines in Figure 6B are the best fits for such kinetics. The model fits the points satisfactorily [compare, for example, with Figure 10 of Zimányi and Lanyi (1993)]. Thus, the agreement between the model and measured data is considerably improved by considering conformational heterogeneity which contributes free energy to the transition states in amounts expected from thermal fluctuations. The distributed kinetics are shown here only for demonstrating their utility; we will give a more detailed account of our experience with distributed and discrete kinetics for the bacteriorhodopsin in another publication.

The fit in Figure 6B shows that at moderately high pH a model containing two N states is required to describe the photocycle (their calculated concentrations are shown with dotted lines). Because the extinction of N is only about 23% less than that of BR, the recovery of BR will be associated with relatively small changes in absorbance. Inasmuch as the recovery of BR from N at high pH should be coincident with the 13-*cis* to all-*trans* reisomerization of retinal, the results predict that all or nearly all of the disappearance of the 350-nm "cis-peak" should occur with the time constant of the slowest, and lowest amplitude, transition observed at 570 nm.

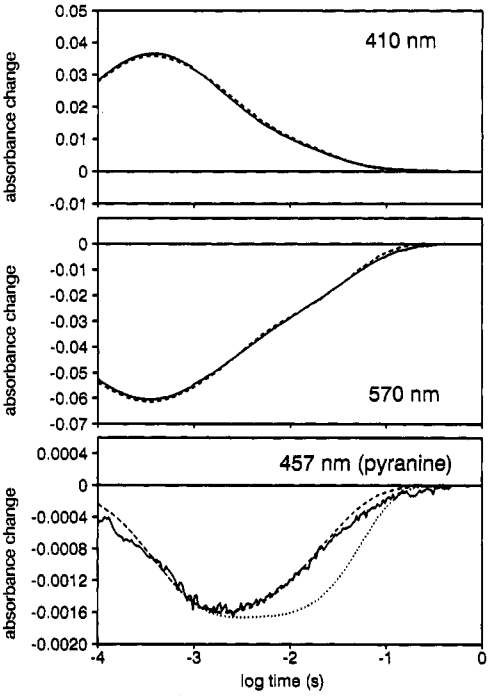


FIGURE 8: Proton release and uptake during the photocycle at moderately high pH. Absorption changes per flash were measured at 410 and 570 nm (with buffer), and at 457 nm (with and without buffer) in the presence of pyranine, as indicated. In the last case, the proton kinetics, i.e., the difference between the traces without and with buffer, are shown. The absorbance decrease at 457 nm corresponds to the pH decrease in the bulk. With the 410- and 570-nm traces, the best fits of the $M_2^{(-1)} \leftrightarrow N^{(-1)} \leftrightarrow N^{(0)} \rightarrow BR$ model are shown (dashed lines), as explained in the test. The rate constants for the $M_2^{(-1)} \rightarrow N^{(-1)}$, $N^{(-1)} \rightarrow M_2^{(-1)}$, $N^{(-1)} \leftrightarrow N^{(0)}$, $N^{(0)} \rightarrow N^{(-1)}$, and $N^{(0)} \rightarrow BR$ reactions were 263, 125, 71, 10, and 33 $s^{-1}$, respectively. With these rate constants, derived from the top and middle panels, two alternatives are calculated for the bottom panel (shown with the 457-nm trace): proton uptake during the decay of the first N state (dashed line); proton uptake during the decay of the second N state (dotted line). For the proton release, an empirical time constant of 450 $\mu$s was used that corresponds approximately to the response of the dye. Conditions: 20 $\mu$M bacteriorhodopsin, 2 M NaCl, 50 $\mu$M pyranine, pH 8.5, 22 °C. When buffer was added, it was Bis-Tris-propane, to a concentration of 20 mM.

This is indeed what had been reported (Dancsházy et al., 1986).

*Proton Uptake Kinetics.* Reprotonation of D96 is thought to take place during the decay of N, but with the two sequential N states required by the above results, we need to reexamine this question. With two N states, proton uptake could occur either in the interconversion of the two N substates or in the final N to BR reaction. Proton exchange between the protein and the bulk was therefore followed with the pH-indicator dye pyranine. Although the $pK_a$ of this dye under the conditions of the experiment is 6.7, we were able to measure the transient pH change during the photocycle at a pH as high as 8.5, which is near the practical limit where the response of the dye is detectable.

The top and middle panels, respectively, of Figure 8 show absorption changes at 410 and 570 nm, which define the time constants needed to calculate the transient concentrations of M and the two N states. These and the extinctions of M and N relative to BR (Figure 6A) were used to obtain fits of the $M_2^{(-1)} \leftrightarrow N^{(-1)} \leftrightarrow N^{(0)} \rightarrow BR$ scheme, as shown with dashed lines. Importantly, the first two time constants in the 570-nm trace are associated with the M $\leftrightarrow$ N reaction, and only the third (at about 100 ms) refers to the N $\rightarrow$ BR conversion. Figure 8 (bottom panel) contains the net pyranine absorption

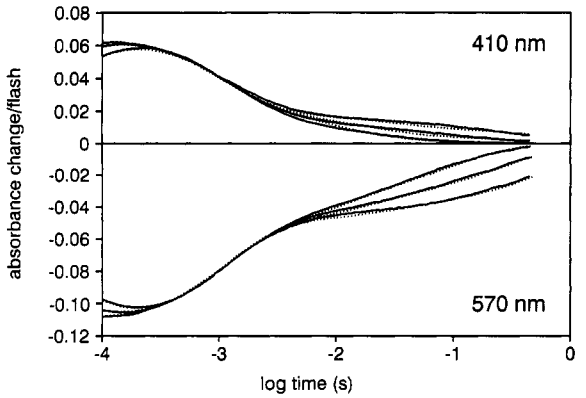


FIGURE 9: Single-wavelength measurements of photocycle kinetics at 410 and 570 nm. Conditions: 16 $\mu$M bacteriorhodopsin, 0.1 M NaCl, 50 mM Bis-Tris-propane or CAPS, 25 °C. The three sets of traces, in the order of increasingly slowed relaxations, were measured at pH 9, 10, and 11. Solid lines, measured absorbances; dashed lines, fits of the model in the text.

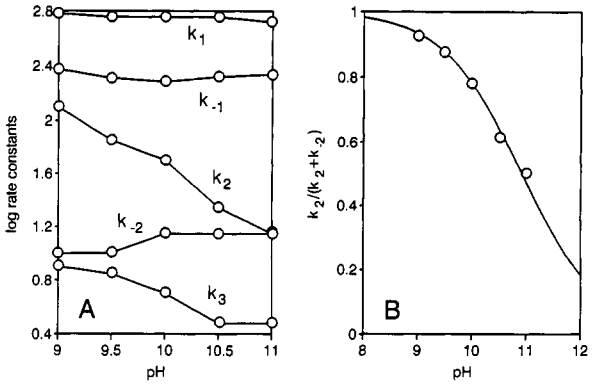


FIGURE 10: Calculated rate constants for the M to BR segment of the photocycle. (*A*) pH dependence of the rates from the fits of the model in Figure 9. The designations $k_1$, $k_{-1}$, $k_2$, $k_{-2}$, and $k_3$ are the rate constants of the $M_2^{(-1)} \rightarrow N^{(-1)}$, $N^{(-1)} \rightarrow M_2^{(-1)}$, $N^{(-1)} \rightarrow N^{(0)}$, $N^{(0)} \rightarrow N^{(-1)}$, and $N^{(0)} \rightarrow$ BR reactions, respectively. (*B*) Estimation of the p$K_a$ for proton exchange with the bulk in the $N^{(-1)} \leftrightarrow N^{(0)}$ equilibrium.

kinetics, which exhibit the usually observed delayed response of this dye to proton release (Grzesiek & Dencher, 1986; Heberle & Dencher, 1990, 1992; Otto et al., 1989, 1990; Cao et al., 1993) on the surface. Proton release is with an apparent time constant of 450 $\mu$s; this is similar to what is reported elsewhere. Uptake is with a time constant of 35 ms, ignoring minor deviations from a single exponential which are within measuring error. Thus, proton uptake takes place well before the recovery of BR. Also shown in the bottom panel of Figure 8 are the more exact predictions of the two models considered: proton uptake during the $N^{(-1)} \rightarrow N^{(0)}$ or during the $N^{(0)} \rightarrow$ BR reaction. The observed pyranine trace clearly agrees with the first of these. Proton uptake from the bulk is therefore described by the scheme $N^{(-1)} + H^+$ (from the bulk) $\rightarrow N^{(0)}$. The proton uptake kinetics in the bottom panel of Figure 8 provide important support to the model for chromophore kinetics in Figure 6B, in that they detect the predicted additional process between the rise and the decay of what analysis of the spectra identified as the first and the second N state, respectively.

*Rate Constants in the M to BR Photocycle Segment for Wild-Type and R227Q Bacteriorhodopsins between pH 9 and 11.* It is implicit in the model we propose that the reaction $N^{(-1)} + H^+$ (from the bulk) $\rightarrow N^{(0)}$ should be dependent on pH while the others need not be. We tested this prediction of the model, although we did so with some hesitation because it is well-known that numerous complications exist above pH 10 which might make these measurements ambiguous. With increasing pH, the spectrum of bacteriorhodopsin shifts somewhat toward the blue, suggesting heterogeneity (Fischer & Oesterhelt, 1979; Druckmann et al., 1982; Balashov et al., 1991; Fukuda & Kouyama, 1992; Brown et al., 1993b), D96 might begin to deprotonate even without photoexcitation (Fukuda & Kouyama, 1992), cooperative effects affect the decay kinetics of M (Tokaji & Dancsházy, 1991, 1992a), and because the relaxations are slower the measuring light might begin to perturb the photocycle kinetics. For these reasons, we regard the results, described below, as approximate only.

The pH dependencies of the rate constants in the $M_2^{(-1)} \leftrightarrow N^{(-1)} \leftrightarrow N^{(0)} \rightarrow$ BR scheme were determined by single-wavelength measurements at 410 and 570 nm. Figure 9 shows measured traces at pH 9, 10, and 11 (solid lines), while the dotted lines are fits of the model. The rate constants from the fits in Figure 9 are shown in Figure 10A. Those in the $M_2^{(-1)} \leftrightarrow N^{(-1)}$ equilibrium are pH-independent, as found previously (Otto et al., 1989; Váró & Lanyi, 1990b; Cao et al., 1991).

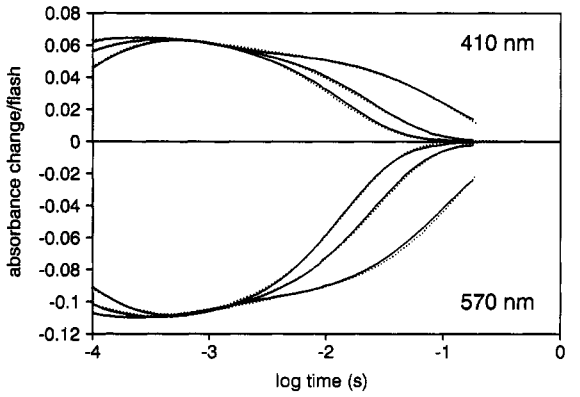


FIGURE 11: Single-wavelength measurements of photocycle kinetics for R227Q bacteriorhodopsin at 410 and 570 nm. Conditions: 22 $\mu$M bacteriorhodopsin, 0.1 M NaCl, 50 mM Bis-Tris-propane or CAPS, 25 °C. The three sets of traces, in the order of increasingly slowed relaxations, were measured at pH 9, 10, and 11. Solid lines, measured absorbances; dashed lines, fits of the model in the text.

The apparent rate constant of the $N^{(-1)} \rightarrow N^{(0)}$ reaction decreases with pH in the way expected if it included proton uptake. The $N^{(0)} \rightarrow N^{(-1)}$ back-reaction is relatively pH-independent, also as expected. For reasons we do not yet understand, the $N^{(0)} \rightarrow$ BR reaction appears to have a somewhat pH-dependent rate (although not in R227Q, cf. Figure 12A).

From the data in Figure 10A, we could calculate the $\Delta pK_a$ between the Schiff base and D96, and the p$K_a$ for proton uptake. From the rate constants in the $M_2^{(-1)} \leftrightarrow N^{(-1)}$ proton-transfer equilibrium, we estimate that the p$K_a$ of D96 is 0.4 pH unit lower at this time than the p$K_a$ of the Schiff base. In Figure 10B, $k_{forward}/(k_{forward} + k_{backward})$ is shown for the $N^{(-1)} \leftrightarrow N^{(0)}$ equilibrium as a function of pH, along with the best fit of a protonation equilibrium for this reaction. Because the surface potential on the cytoplasmic side of the protein has a profound effect on the local pH, the apparent number of protons is less than 1 (Miller & Oesterhelt, 1990; Holz et al., 1989; Tittor et al., 1989; Cao et al., 1991). In Figure 10B, 0.6 proton was used. The p$K_a$ associated with proton uptake is approximately 11.

Figure 11 shows absorption changes at 410 and 570 nm in the R227Q protein (solid lines) at pH 9, 10, and 11. As for the data with wild-type in Figure 9, the model was fitted to these traces (dotted lines). Figure 12A shows the rate constants of this fit as functions of the pH; Figure 12B gives

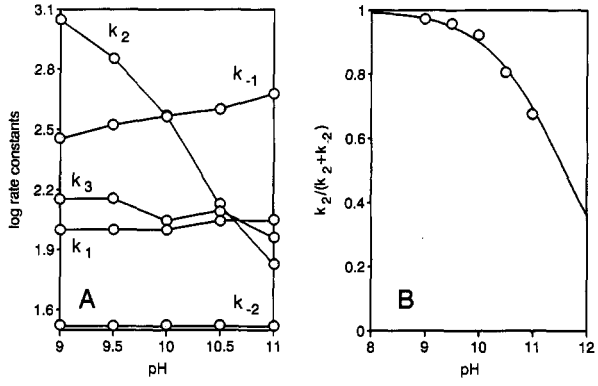


FIGURE 12: Calculated rate constants for the M to BR segment of the photocycle of R227Q bacteriorhodopsin. (*A*) pH dependence of the rates from the fits of the model in Figure 11. The designations $k_1$, $k_{-1}$, $k_2$, $k_{-2}$, and $k_3$ are as in Figure 10. (*B*) Estimation of the p$K_a$ for proton exchange with the bulk in the $N^{(-1)} \leftrightarrow N^{(0)}$ equilibrium.

the function which defines the p$K_a$ associated with proton uptake. This p$K_a$ is about 11.5, i.e., somewhat increased over the value in wild-type (cf. Figure 10B). The most significant changes from wild-type are the following: (a) The equilibrium constant $K = [M_2^{(-1)}]/[N^{(-1)}]$ is shifted from 0.4 in wild-type to 3.4 in R227Q. This means that in R227Q the p$K_a$ of D96 is about 0.5 pH unit *higher* than that of the Schiff base at this time in the photocycle, rather than 0.4–0.6 unit lower. (b) The rate constants in the $N^{(-1)} + H^+$ (from the bulk) $\leftrightarrow N^{(0)}$ reaction are both about an order of magnitude faster than in wild-type. Thus, proton exchange between the protein and the bulk is strongly accelerated upon replacement of R227. This might be the result of removing the positive charge of R227. (c) The $N^{(0)} \rightarrow$ BR reaction is nearly 20 times faster than in wild-type. (d) Because the $M_2^{(-1)} \rightarrow N^{(-1)}$ reaction is slower and the $N^{(-1)} \rightarrow N^{(0)}$ reaction is faster than wild-type, $N^{(-1)}$ accumulates in much smaller amounts, consistent with the decreased N to M back-reaction found in the two-flash experiments (Figure 4B).

## DISCUSSION

The results we report provide strong evidence for the scheme $M_2^{(-1)} \leftrightarrow N^{(-1)} \leftrightarrow N^{(0)} \rightarrow$ BR as the description of the M to BR pathway at pH >8.5, and for proton uptake from the bulk in the $N^{(-1)} \rightarrow N^{(0)}$ step. The two-flash experiments (Figures 1–3) confirm the findings which demonstrated the existence of significant $N^{(-1)} \rightarrow M_2^{(-1)}$ back-reaction (Druckmann et al., 1993), and rule out alternative schemes with two parallel M states of different decay rates (e.g., Hanamoto et al., 1984; Diller & Stockburger, 1988; Dancsházy et al., 1988; Bitting et al., 1990; Tokaji & Dancsházy, 1992b) under the conditions of these experiments. The kinetics of M and N as calculated from time-resolved spectra (Figures 5–7) accommodate the thermal back-reaction only with two sequential N states. Indeed, the uptake of the transported proton (Figure 8, bottom panel) occurs after the decay of M but well before the recovery of BR, and has the time constant calculated for the decay of the first N. The existence of two such sequential N states had been suggested on the basis of the pH dependence of the N to O reaction (Ames & Mathies, 1990). That we could resolve them demonstrates that proton uptake (decay of the predicted first N) and 13-cis to all-trans reisomerization of the retinal (decay of the predicted second N) need not occur simultaneously.

Since $N^{(-1)}$ differs from $N^{(0)}$ in protonation state and proton uptake on the cytoplasmic side at this time in the photocycle will reprotonate D96, the simplest interpretation of the proposed scheme is that the $N^{(-1)} \rightarrow N^{(0)}$ reaction represents the reprotonation of D96. This would predict that at pH >8.5 at least, a late N state should be found where the 1742-cm$^{-1}$ negative FTIR band due to the deprotonated D96 is absent but the fingerprint region still contains evidence for the 13-cis isomeric state of the retinal. So far, no such resolution of N into substates is evident in reported FTIR data. Whether the observed proton uptake before the recovery of BR reprotonates D96 directly or indirectly from another group remains, therefore, open.

In BR, the p$K_a$ of D96 and the Schiff base are both above 9 or 10 (Engelhard et al., 1985; Gerwert et al., 1989; Braiman et al., 1991; Pfefferlé et al., 1991; Maeda et al., 1992), but during the $L \rightarrow M_1$ reaction the Schiff base p$K_a$ will have strongly decreased to allow proton transfer to the low-p$K_a$ residue D85. Yet the rate constants for the $M_2^{(-1)} \leftrightarrow N^{(-1)}$ internal proton transfer in this and an earlier paper (Cao et al., 1991) indicate that at this time in the photocycle the p$K_a$ difference between the Schiff base and D96 is overcome and the p$K_a$ of the Schiff base is now 0.4–0.6 pH unit *higher* than that of D96. Elsewhere we report that in the blue form of the D212N mutant D96 releases its proton to the bulk even though the Schiff base does not deprotonate in its photocycle (Cao et al., 1993). This occurs at a pH as low as 7, suggesting that the p$K_a$ of D96 is strongly decreased. It was argued that a similarly large decrease in the proton affinity of D96 occurs in the photocycle of the wild-type protein also, and that it is part of the reason for the reprotonation of the Schiff base. Increased interaction with R227 in $M_2^{(-1)}$ could account for at least part of the decreased proton affinity of D96 (Stern & Khorana, 1989). Indeed, in the R227Q protein, the p$K_a$ of D96 is about 0.5 pH unit *higher* than that of the Schiff base rather than 0.4–0.6 unit lower as in wild-type (cf. rate constants in Figures 10A and 12A). Thus, it would appear that stabilization of the anionic form of D96 by increased Coulombic interaction with the positive charge of R227 is responsible for an about 1 pH unit decrease of the p$K_a$ of D96 in $M_2^{(-1)}$. The rest of the postulated p$K_a$ decrease is probably related to the earlier described effects of bound water near D96 (Cao et al., 1991) on the proton transfer to the Schiff base.

The problem is that these results reveal only the changes in the p$K_a$s and the $\Delta$p$K_a$ between D96 and the Schiff base, rather than their absolute values. An actual p$K_a$ can be determined only from the rates in the $N^{(-1)} \leftrightarrow N^{(0)}$ equilibration which follows the reprotonation of the Schiff base. These indicate that the proton uptake on the cytoplasmic side is by a group with a p$K_a$ of approximately 11. This p$K_a$ is also somewhat influenced by R227 since its replacement with glutamine raises it by about 0.5 pH unit (Figures 10B and 12B). It may or may not be the p$K_a$ of D96, since we do not know whether the reprotonation of D96 is directly from the bulk. Nevertheless, it would seem that if the p$K_a$ of D96 is indeed lowered in $M_2^{(-1)}$ as we suggest, the high p$K_a$ detected means that it will rise to its initial value above 10 in $N^{(-1)}$ or $N^{(0)}$.

We had reported earlier (Zimányi et al., 1992) that the proton *release* on the extracellular side is from a group with a p$K_a$ of about 6. We find now that proton *uptake* on the cytoplasmic side is by a group with a p$K_a$ of about 11. These determined proton affinities for release and uptake provide insights into the energetics of the proton pump. The results indicate that bacteriorhodopsin generates a transmembrane proton electrochemical potential by releasing a proton on one side from a group with low proton affinity and taking up a

proton on the other side to protonate a group with high proton affinity. The difference in the p$K_a$s of the release and uptake groups is about 5 pH units. An affinity difference of this magnitude should enable the pump to transport protons against an electrochemical gradient of 5 × 60 = 300 mV. This is equivalent to about 30 kJ/mol. The rest of the excess 50 kJ/mol in the K intermediate, dissipated mainly in the $M_1 \rightarrow M_2$ and the O → BR reactions (Váró & Lanyi, 1991b; Zimányi et al., 1992), is evidently used to compensate for thermal losses in resetting the system in each turnover of the photocycle.

## APPENDIX

In model A represented by M ↔ N → BR, $k_1$, $k_{-1}$, and $k_2$ are the rate constants of the M → N, N → M, and N → BR reactions, respectively. At $t = 0$, $M(t) = 1$ and $N(t) = 0$. At $t = t_p$, the reaction is perturbed with the second flash which decreases $M(t)$ by $\Delta M$, while $N(t)$ is not significantly changed. Thus, at $t > t_p$

$$M(t) = M_A(t) + M_B(t) \quad (1)$$

where $M_A(t)$ is the M concentration as it would be without the perturbation, and $M_B(t)$ is the (additive) consequence of the perturbation. For the case where $k_{-1} \neq 0$, $M_A(t)$ is given by the analytical solution of the rate equations:

$$M_A(t) = \frac{1}{K_1 - K_2}\left[\left(\frac{K_1K_2}{k_2} - K_2\right)\exp(-K_1t) - \left(\frac{K_1K_2}{k_2} - K_1\right)\exp(-K_2t)\right] \quad (2)$$

and the net effect of the perturbation is

$$M_B(t) = -\Delta M[M_A(t - t_p)] \quad (3)$$

where $K_1 = p + q$, $K_2 = p - q$, $p = 1/2(k_1 + k_{-1} + k_2)$, and $q = (p^2 - k_1k_2)^{1/2}$.

Thus, the perturbed *minus* control difference kinetics will have the same time course (shifted by $t_p$), but decreasing amplitude with increasing time, as the unperturbed control kinetics.

Model B contains no back-reaction but two or more independent M states each with a decay rate constant $k_i$ and a quantum yield of blue light reconversion $\phi_i$. $M(t)$ is described by the equations:

$$M(t) = \sum\{\exp(-k_it) - \phi_i\Delta M \exp[-k_i(t - t_p)]\} \quad (4)$$

or

$$M(t) = \sum\{[1 - \phi_i\Delta M \exp(k_it_p)]\exp(-k_it)\} \quad (5)$$

If back-reactions are allowed for several, e.g., two, independently decaying M states, there will be two sets of rate constants, $k_1^f$, $k_{-1}^f$, and $k_2^f$ and $k_1^s$, $k_{-1}^s$, and $k_2^s$, where the superscripts f and s refer to the faster and slower decaying M states, $M_{fast}$ and $M_{slow}$. Additional parameters of relevance are $c^f$ and $c^s$ and $\phi^f$ and $\phi^s$, which are the initial amounts and reconversion quantum yields of $M_{fast}$ and $M_{slow}$, respectively. Here, $\Delta M$ has two components: $\Delta M^f = \phi^f c^f M_A^f(t_p)$ and $\Delta M^s = \phi^s c^s M_A^s(t_p)$; hence, the net consequence of the perturbation is

$$M_B(t) = -[\phi^f c^f M_A^f(t_p)M_A^f(t - t_p) + \phi^s c^s M_A^s(t_p)M_A^s(t - t_p)] \quad (6)$$

In this model, $M_B(t)$ will be dependent on $t_p$, i.e., the time when the perturbation is applied. This is because $M_A^f(t - t_p)$ and $M_A^s(t - t_p)$ are perforce different functions. As $t_p$ is shifted to longer times, $M_A^f(t_p)$ will have decreased faster than $M_A^s(t_p)$; therefore, the weight of $M_A^f(t - t_p)$ will be less and less relative to $M_A^s(t - t_p)$, gradually changing the overall kinetics of $M_B(t)$.

## REFERENCES


Ames, J. B., & Mathies, R. A. (1990) *Biochemistry 29*, 7181–7190.

Balashov, S. P., Imasheva, E. S., Litvin, F. F., & Lozier, R. H. (1990) *FEBS Lett. 271*, 93–96.

Balashov, S. P., Govindjee, R., & Ebrey, T. G. (1991) *Biophys. J. 60*, 475–490.

Bitting, H. C., Jang, D.-J., & El-Sayed, M. A. (1990) *Photochem. Photobiol. 51*, 593–598.

Braiman, M. S., Mogi, T., Marti, T., Stern, L. J., Khorana, H. G., & Rothschild, K. J. (1988) *Biochemistry 27*, 8516–8520.

Braiman, M. S., Bousché, O., & Rothschild, K. J. (1991) *Proc. Natl. Acad. Sci. U.S.A. 88*, 2388–2392.

Brown, L. S., Bonet, L., Needleman, R., & Lanyi, J. K. (1993a) *Biophys. J.* (in press).

Brown, L. S., Zimányi, L., Needleman, R., Ottolenghi, M., & Lanyi, J. K. (1993b) *Biochemistry* (following paper in this issue).

Cao, Y., Váró, G., Chang, M., Ni, B., Needleman, R., & Lanyi, J. K. (1991) *Biochemistry 30*, 10972–10979.

Cao, Y., Váró, G., Klinger, A. L., Czajkowsky, D. M., Braiman, M. S., Needleman, R., & Lanyi, J. K. (1993) *Biochemistry 32*, 1981–1990.

Chernavskii, D. S., Chizhov, I. V., Lozier, R. H., Murina, T. M., Prokhorov, A. M., & Zubov, B. V. (1989) *Photochem. Photobiol. 49*, 649–653.

Chizhov, I., Engelhard, M., Chernavskii, D. S., Zubov, B., & Hess, B. (1992) *Biophys. J. 61*, 1001–1006.

Dancsházy, Z., Govindjee, R., Nelson, B., & Ebrey, T. G. (1986) *FEBS Lett. 209*, 44–48.

Dancsházy, Z., Govindjee, R., & Ebrey, T. G. (1988) *Proc. Natl. Acad. Sci. U.S.A. 85*, 6358–6361.

Diller, R., & Stockburger, M. (1988) *Biochemistry 27*, 7641–7651.

Druckmann, S., Ottolenghi, M., Pande, A., Pande, J., & Callender, R. H. (1982) *Biochemistry 21*, 4953–4959.

Druckmann, S., Friedman, N., Lanyi, J. K., Needleman, R., Ottolenghi, M., & Sheves, M. (1992) *Photochem. Photobiol. 56*, 1041–1047.

Druckmann, D., Heyn, M. P., Lanyi, J. K., Ottolenghi, M., & Zimányi, L. (1993) *Biophys. J.* (in press).

Eisfeld, W., & Stockburger, M. (1992) in *Structures and Functions of Retinal Proteins* (Rigaud, J. L., Ed.) pp 139–142, John Libbey Eurotext Ltd., Montrouge, France.

Engelhard, M., Gerwert, K., Hess, B., Kreutz, W., & Siebert, F. (1985) *Biochemistry 24*, 400–407.

Fischer, U., & Oesterhelt, D. (1979) *Biophys. J. 28*, 211–230.

Fukuda, K., & Kouyama, T. (1992a) *Photochem. Photobiol. 56*, 1057–1062.

Fukuda, K., & Kouyama, T. (1992b) *Biochemistry 31*, 11740–11747.

Gerwert, K., Hess, B., Soppa, J., & Oesterhelt, D. (1989) *Proc. Natl. Acad. Sci. U.S.A. 86*, 4943–4947.

Gerwert, K., Souvignier, G., & Hess, B. (1990) *Proc. Natl. Acad. Sci. U.S.A. 87*, 9774–9778.

Groma, G. I., & Dancsházy, Z. (1986) *Biophys. J. 50*, 357–366.

Grzesiek, S., & Dencher, N. A. (1986) *FEBS Lett. 208*, 337–342.

Hanamoto, J. H., Dupuis, P., & El-Sayed, M. A. (1984) *Proc. Natl. Acad. Sci. U.S.A. 81*, 7083–7087.

Heberle, J., & Dencher, N. A. (1990) *FEBS Lett. 277*, 277–280.

Heberele, J., & Dencher, N. A. (1992) *Proc. Natl. Acad. Sci. U.S.A. 89*, 5996–6000.

Henderson, R., Baldwin, J. M., Ceska, T. A., Zemlin, F., Beckmann, E., & Downing, K. H. (1990) *J. Mol. Biol. 213*, 899–929.

Holz, M., Lindau, M., & Heyn, M. P. (1988) *Biophys. J. 53*, 623–633.
Holz, M., Drachev, L. A., Mogi, T., Otto, H., Kaulen, A. D., Heyn, M. P., Skulachev, V. P., & Khorana, H. G. (1989) *Proc. Natl. Acad. Sci. U.S.A. 86*, 2167–2171.
Kalisky, O., Lachish, U., & Ottolenghi, M. (1978) *Photochem. Photobiol. 28*, 261–263.
Kalisky, O., Ottolenghi, M., Honig, B., & Korenstein, R. (1981) *Biochemistry 20*, 649–655.
Kouyama, T., Nasuda-Kouyama, A., Ikegami, A., Mathew, M. K., & Stoeckenius, W. (1988) *Biochemistry 27*, 5855–5863.
Lanyi, J. K. (1992) *J. Bioenerg. Biomembr. 24*, 169–179.
Lin, G. C., El-Sayed, M. A., Marti, T., Stern, L. J., Mogi, T., & Khorana, H. G. (1991) *Biophys. J. 60*, 172–178.
Maeda, A., Sasaki, J., Shichida, Y., Yoshizawa, T., Chang, M., Ni, B., Needleman, R., & Lanyi, J. K. (1992) *Biochemistry 31*, 4684–4690.
Mathies, R. A., Lin, S. W., Ames, J. B., & Pollard, W. T. (1991) *Annu. Rev. Biophys. Biophys. Chem. 20*, 491–518.
Miller, A., & Oesterhelt, D. (1990) *Biochim. Biophys. Acta 1020*, 57–64.
Needleman, R., Chang, M., Ni, B., Váró, G., Fornes, J., White, S. H., & Lanyi, J. K. (1991) *J. Biol. Chem. 266*, 11478–11484.
Ni, B., Chang, M., Duschl, A., Lanyi, J. K., & Needleman, R. (1990) *Gene 90*, 169–172.
Oesterhelt, D., & Stoeckenius, W. (1974) *Methods Enzymol. 31*, 667–678.
Oesterhelt, D., Tittor, J., & Bamberg, E. (1992) *J. Bioenerg. Biomembr. 24*, 181–191.
Ohtani, H., Itoh, H., & Shinmura, T. (1992) *FEBS Lett. 305*, 6–8.
Otto, H., Marti, T., Holz, M., Mogi, T., Lindau, M., Khorana, H. G., & Heyn, M. P. (1989) *Proc. Natl. Acad. Sci. U.S.A. 86*, 9228–9232.
Otto, H., Marti, T., Holz, M., Mogi, T., Stern, L. J., Engel, F., Khorana, H. G., & Heyn, M. P. (1990) *Proc. Natl. Acad. Sci. U.S.A. 87*, 1018–1022.
Pfefferlé, J.-M., Maeda, A., Sasaki, J., & Yoshizawa, T. (1991) *Biochemistry 30*, 6548–6556.
Rothschild, K. J. (1992) *J. Bioenerg. Biomembr. 24*, 147–167.
Skulachev, V. P., Drachev, L. A., Kaulen, A. D., & Zorina, V. V. (1988) in *Molecular Physiology of Retinal Proteins* (Hara, T., Ed.) pp 117–123, Yamada Science Foundation, Osaka, Japan.
Souvignier, G., & Gerwert, K. (1992) *Biophys. J. 63*, 1393–1405.
Stern, L. J., & Khorana, H. G. (1989) *J. Biol. Chem. 264*, 14202–14208.
Tittor, J., Soell, C., Oesterhelt, D., Butt, H.-J., & Bamberg, E. (1989) *EMBO J. 8*, 3477–3482.
Tokaji, Z., & Dancsházy, Z. (1991) *FEBS Lett. 281*, 170–172.
Tokaji, Z., & Dancsházy, Z. (1992a) in *Structures and Functions of Retinal Proteins* (Rigaud, J. L., Ed.) pp 175–178, John Libbey Eurotext Ltd., Montrouge, France.
Tokaji, Z., & Dancsházy, Z. (1992b) *FEBS Lett. 311*, 267–270.
Váró, G., & Keszthelyi, L. (1983) *Biophys. J. 43*, 47–51.
Váró, G., & Lanyi, J. K. (1990a) *Biochemistry 29*, 6858–6865.
Váró, G., & Lanyi, J. K. (1990b) *Biochemistry 29*, 2241–2250.
Váró, G., & Lanyi, J. K. (1991a) *Biochemistry 30*, 5008–5015.
Váró, G., & Lanyi, J. K. (1991b) *Biochemistry 30*, 5016–5022.
Váró, G., Zimányi, L., Chang, M., Ni, B., Needleman, R., & Lanyi, J. K. (1992) *Biophys. J. 61*, 820–826.
Yamamoto, N., Naramoto, S., & Ohtani, H. (1992) *FEBS Lett. 314*, 345–347.
Zimányi, L., & Lanyi, J. K. (1993) *Biophys. J. 64*, 240–251.
Zimányi, L., Keszthelyi, L., & Lanyi, J. K. (1989) *Biochemistry 28*, 5165–5172.
Zimányi, L., Váró, G., Chang, M., Ni, B., Needleman, R., & Lanyi, J. K. (1992) *Biochemistry 31*, 8535–8543.